INT. J. NUM. METH. HEAT FLUID FLOW, VOL. 2, 63–78 (1992)

GAS FLOW IN A SINGLE CYLINDER INTERNAL COMBUSTION ENGINE: A MODEL AND ITS NUMERICAL TREATMENT

GABRIELE ENGL AND PETER RENTROP

Mathematisches Institut, Technische Universität München, Arcisstr. 21, Postfach 202420, D-8000 München 2, Germany

ABSTRACT

We present results of a mathematical model for the gas flow in an internal combustion engine consisting of a single cylinder with an inlet and outlet pipe. In order to achieve optimal performance of the engine the dependence of the gas flow on physical parameters such as pipe dimensions and valve geometry need to be understood. A system of ordinary differential equations (in time t) with discontinuous right-hand side describes the gas properties in the cylinder, whereas the gas flow in each pipe is modelled by the Euler equations, a system of hyperbolic partial differential equations. The explicit method of Euler and a TVD scheme are used for solving these equations. However, since the coupling of the pipe equations with the o.d.e. system in the cylinder on one side and atmospheric gas properties on the other appeared to be a main problem, we concentrate on appropriate coupling conditions. The numerical techniques involve discretization in space and time, and we present different methods of discrete coupling. As a main result we show that the various coupling methods lead to quite different numerical solutions. Therefore, a careful treatment of the coupling conditions is crucial.

KEY WORDS Internal combustion engine Euler equations TVD method Boundary conditions Coupling conditions

INTRODUCTION

We consider a four-stroke cycle internal combustion engine consisting of a single cylinder, inlet and outlet pipe and two valves connecting the cylinder with the pipes, as shown in *Figure 1.*

One four-stroke cycle includes combustion cycle and charge cycle. During the latter the burnt gas is replaced by a fresh fuel–air mixture. The gas exchange is controlled by the movement of inlet and outlet valves and is strongly affected by their geometrical shape.

Optimal performance of an internal combustion engine is of great interest and requires the complete replacement of the burnt gas during the charge cycle. In order to support the gas exchange it is essential to open the inlet valve when there is high pressure in the inlet pipe and to open the outlet valve when there is low pressure in the outlet pipe.

The original problem can be classified as an 'inverse problem': how should specified technical parameters, e.g. the diameter of the pipe and the geometry of the valves, be chosen in order to achieve an optimal charge cycle?

In the following we treat the 'simulation problem' for the simplified model: atmosphere–cylinder (o.d.e. system)–inlet pipe (gas equations)–atmosphere. A mathematical modelling of the outlet pipe can be carried out in analogy to the inlet pipe.

MATHEMATICAL MODEL

The time dependency of mass m_Z, temperature T_Z and pressure p_Z of the gas in the cylinder is described. Within the inlet pipe we study the time dependency of the gas density ρ_E, velocity

0961–5539/92/010063–16$2.00

Received March 1991
Revised September 1991

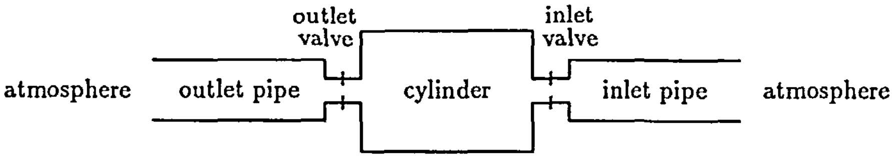

Figure 1 Model of internal combustion engine

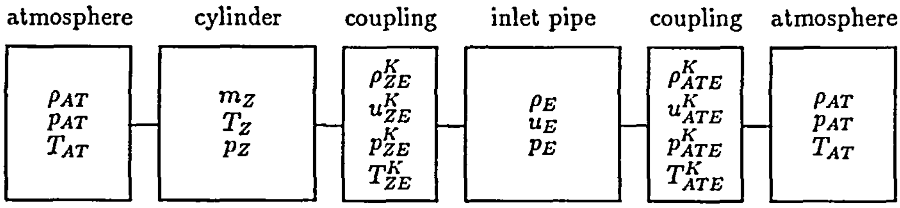

Figure 2 Scheme of the coupled systems

u_E and pressure p_E (ρ_E, u_E and p_E are also dependent on space x). The atmospheric gas values ρ_{AT}, p_{AT} and T_{AT} are known. Furthermore the systems cylinder and inlet pipe as well as inlet pipe and atmosphere have to be coupled, and the upper index 'K' denotes the coupling quantities. A scheme of the coupled systems is shown in *Figure 2.*

Cylinder equations

Figure 3 shows the geometry of the cylinder. l, r and H are given geometric constants. The crank angle φ is a function of time t: $\varphi = \omega t$, where ω denotes the angular frequency. The cylinder volume V_Z and the distance s are functions of φ (and therefore functions of t):

$$V_Z = V_Z(\varphi) = \tfrac{1}{2} V_H \left[\frac{\varepsilon+1}{\varepsilon-1} - \cos\varphi + \frac{1}{\lambda}\left(1 - \sqrt{1-(\lambda \sin\varphi)^2}\right) \right]$$

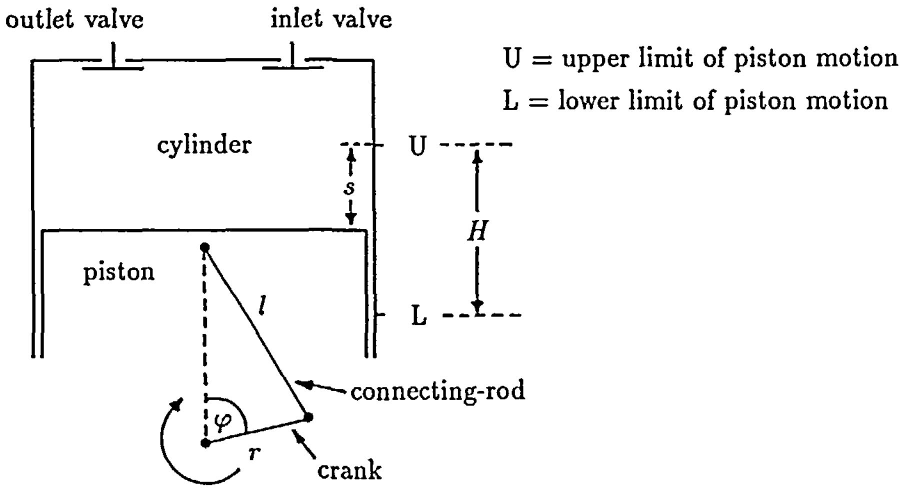

Figure 3 Cylinder geometry

$$s=s(\varphi)=r\left[1-\cos\varphi+\frac{1}{\lambda}\left(1-\sqrt{1-(\lambda\sin\varphi)^2}\right)\right]$$

where V_H, ε and λ are given physical parameters.

The original three-dimensional hydrodynamical problem of the gas flow in the cylinder is simplified by neglecting the dependence on spatial dimensions and assuming an ideal gas, which does not change its thermodynamical properties during the combustion cycle. Mass balance and energy balance yield a system of two ordinary differential equations in time t for mass m_Z and temperature T_Z:

$$\frac{dm_Z}{dt}=\frac{dm_E}{dt}+\frac{dm_A}{dt}+\frac{dm_B}{dt} \tag{1}$$

$$\frac{dT_Z}{dt}=\frac{1}{m_Z c_v}\left(-p_Z\frac{dV_Z}{dt}+\frac{dm_E}{dt}h_E+\frac{dm_A}{dt}h_A+\frac{dQ_B}{dt}-\frac{dQ_W}{dt}-c_vT_Z\frac{dm_Z}{dt}\right) \tag{2}$$

The pressure p_Z is given by the ideal gas law:

$$p_Z=\frac{Rm_ZT_Z}{V_Z} \tag{3}$$

We use the notations:

m_E/m_A	mass flowing through inlet/outlet valve
m_B	mass of fuel
h_E/h_A	enthalpy which is added or removed through inlet/outlet valve
Q_B	combustion energy
Q_W	heat loss caused by heat exchange with the cylinder surface

c_v, c_p, κ and R are thermodynamic constants:

c_v/c_p	specific heat capacity for constant volume/pressure
$\kappa=c_p/c_v$	ratio of the specific heat capacities
R	universal gas constant

The right-hand side of the o.d.e. system (1), (2) depends on geometric and experimental data and partly discontinuous empirical functions as summarized in the following.

Geometry of the valves. The cross-sectional area $A_{E/A}(t)$ of the inlet/outlet valve opening is given by:

$$A_{E/A}(t)=d_{E/A}vh_{E/A}(\omega t)\pi\sin\beta \tag{4}$$

where the distances d_E, d_A and the angle β are known, and vh_E, vh_A are functions of t as shown in *Figures 4* and *5*.

Mass flow through the valves. The mass flow through the valves is dependent on the cross-sections, A_E and A_A, of the valve openings:

$$\frac{dm_E}{dt}=-\rho^K_{ZE}u^K_{ZE}A_E \tag{5}$$

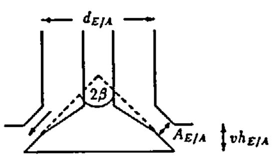

Figure 4 Valve geometry

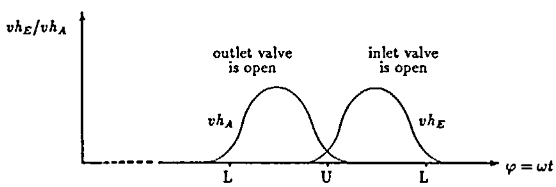

Figure 5 Valve opening and closing

$$\frac{\mathrm{d}m_A}{\mathrm{d}t}=\begin{cases}-A_A\sqrt{2\rho_Z p_Z}\cdot\psi(p_{AT},p_Z) & \text{for } p_Z\geqslant p_{AT}\\ A_A\sqrt{2\rho_{AT}p_{AT}}\cdot\psi(p_Z,p_{AT}) & \text{for } p_Z<p_{AT}\end{cases}\tag{6}$$

where $\rho_Z=m_Z/V_Z$ denotes the gas density in the cylinder and

$$\psi(p_1,p_2)=\begin{cases}\left[\frac{\kappa}{\kappa-1}\left(\left(\frac{p_1}{p_2}\right)^{2/\kappa}-\left(\frac{p_1}{p_2}\right)^{(\kappa+1)/\kappa}\right)\right]^{1/2} & \text{for } \frac{p_1}{p_2}>\left(\frac{2}{\kappa+1}\right)^{\kappa/(\kappa-1)}\\ \left(\frac{2}{\kappa+1}\right)^{1/(\kappa-1)}\left(\frac{\kappa}{\kappa+1}\right)^{1/2} & \text{for } \frac{p_1}{p_2}\leqslant\left(\frac{2}{\kappa+1}\right)^{\kappa/(\kappa-1)}\end{cases}\tag{7}$$

Enthalpies. For simplification we assume an ideal gas and obtain:

$$h_E=\begin{cases}c_pT_Z & \text{for } \frac{\mathrm{d}m_E}{\mathrm{d}t}\leqslant 0\\ c_pT_{ZE}^K+\frac{(u_{ZE}^K)^2}{2} & \text{else}\end{cases}\tag{8}$$

$$h_A=\begin{cases}c_pT_Z & \text{for } \frac{\mathrm{d}m_A}{\mathrm{d}t}\leqslant 0\\ c_pT_{AT}+\frac{1}{2}\left(\frac{(\mathrm{d}m_A/\mathrm{d}t)V_Z}{A_Am_Z}\right)^2 & \text{else}\end{cases}\tag{9}$$

Heat loss at the cylinder surface. The heat exchange between gas and cylinder surface is described by:

$$\frac{\mathrm{d}Q_W}{\mathrm{d}t}=\alpha A_Z(T_Z-T_W)\tag{10}$$

A_Z denotes the cylinder surface and T_W the average surface temperature. A formula for the approximate computation of the heat transfer parameter α is taken from Woschni[19]:

$$\alpha=0.013d^{-0.2}T_Z^{-0.53}p_Z^{0.8}\left[C_1c_m+C_2\frac{V_HT_1}{p_1V_1}(p_Z-p_0)\right]^{0.8}\tag{11}$$

where

d	cylinder diameter
c_m	average velocity of the piston
p_Z-p_0	difference of pressures during combustion (p_Z) and without combustion energy (p_0)
p_1, T_1, V_1	pressure, temperature and volume of a known gas state during compression (e.g. at the time when the inlet valve closes)
C_1, C_2	constants

Combustion. There is no simple analytical way to describe the combustion process and to compute $\mathrm{d}Q_B/\mathrm{d}t$ (Q_B: combustion heat). We use an empirical function describing the so called Wiebe combustion process, see Woschni[18]:

$$\frac{\mathrm{d}Q_B}{\mathrm{d}t}=\frac{m_{B_0}}{t_0}H_u6.9(m+1)\left(\frac{t-t_B}{t_0}\right)^m\exp\left(-6.9\left(\frac{t-t_B}{t_0}\right)^{m+1}\right)\tag{12}$$

for $0\leqslant t-t_B\leqslant t_0$, else $\mathrm{d}Q_B/\mathrm{d}t=0$, where

H_u	heating value
m_{B_0}	total fuel mass (burnt during one combustion cycle)

t_0 total time of combustion
t_B time at which combustion starts
m formal parameter, e.g. $m=1$

Summarizing we can state: the right-hand side of the o.d.e. system (1), (2) is quite complex and can be rewritten as:

$$\frac{dm_Z}{dt}=M(t,m_Z,T_Z,k_{ZE}) \tag{13}$$

$$\frac{dT_Z}{dt}=T(t,m_Z,T_Z,k_{ZE}) \tag{14}$$

where

$$k_{ZE}=(\rho^K_{ZE},u^K_{ZE},p^K_{ZE},T^K_{ZE})$$

denotes a vector of the coupling quantities. M and T are discontinuous functions depending on experimental parameters and empirical functions. The discontinuities are caused by the mathematical model and not by the physical process. The advantage of the mixed theoretical–empirical model (13), (14) is its simplicity compared to the complete Navier–Stokes equations by which chemical reactions for a complex geometry are taken into account. The compact model (13), (14) can be studied more easily to have a realistic prediction of parameter changes. Note that the dependence of M and T on the coupling quantities involves dependence on pipe values. The pressure p_Z is given by (3):

$$p_Z=\frac{Rm_ZT_Z}{V_Z}$$

Pipe equations

The gas flow within the inlet pipe is described for the unsteady, one-dimensional, compressible and non-isentropic case which is modelled by the Euler equations of gas dynamics, a hyperbolic system of partial differential equations for density ρ, velocity u and pressure p (the subscript 'E' for the pipe values is omitted in the following):

$$\begin{aligned}
&\rho_t+\rho u_x+u\rho_x=-\rho\frac{A_t}{A}-\rho u\frac{A_x}{A}\\
&u_t+uu_x+\frac{1}{\rho}p_x=0\\
&p_t+\kappa p u_x+up_x=-p\frac{A_t}{A}-\kappa p u\frac{A_x}{A}
\end{aligned} \tag{15}$$

where $A=A(x,t)$ denotes the cross-sectional area of the pipe[2,8,10,11].

In the following we simplify our model by restricting the pipe to a constant cross-section. System (15) reduces to:

$$\frac{\partial}{\partial t}\begin{pmatrix}\rho\\u\\p\end{pmatrix}+\begin{pmatrix}u & \rho & 0\\ 0 & u & \frac{1}{\rho}\\ 0 & \kappa p & u\end{pmatrix}\frac{\partial}{\partial x}\begin{pmatrix}\rho\\u\\p\end{pmatrix}=0 \tag{16}$$

For the treatment of the coupling conditions the characteristic form of (16) is useful. The characteristic directions (eigenvalues of the matrix in (16)) are given by:

$$\frac{\mathrm{d}x}{\mathrm{d}t}=u+a, \qquad \frac{\mathrm{d}x}{\mathrm{d}t}=u-a \qquad \text{and} \qquad \frac{\mathrm{d}x}{\mathrm{d}t}=u \tag{17}$$

where $a=\sqrt{\kappa(p/\rho)}\neq 0$ (sound speed), and hence (16) is equivalent to:

$$\begin{aligned}(p_t+(u+a)p_x)+\rho a(u_t+(u+a)u_x)&=0\\ (p_t+(u-a)p_x)-\rho a(u_t+(u-a)u_x)&=0\\ (p_t+up_x)-a^2(\rho_t+u\rho_x)&=0\end{aligned} \tag{18}$$

System (16) can also be rewritten as a system of conservation laws:

$$\frac{\partial U}{\partial t}+\frac{\partial F(U)}{\partial x}=0 \tag{19}$$

where

$$U=\begin{pmatrix}\rho\\ e\\ m\end{pmatrix}, \qquad F=\begin{pmatrix} m\\ \dfrac{\kappa em}{\rho}-\tfrac{1}{2}(\kappa-1)\dfrac{m^3}{\rho^2}\\ (\kappa-1)e-\tfrac{1}{2}(\kappa-3)\dfrac{m^2}{\rho}\end{pmatrix}$$

and $e=\frac{1}{2}\rho u^2+\dfrac{p}{\kappa-1}$ energy per unit volume

$m=\rho u$ momentum per unit volume

or equivalently

$$\frac{\partial U}{\partial t}+A(U)\frac{\partial U}{\partial x}=0 \tag{20}$$

where

$$A(U)=\frac{\mathrm{d}F(U)}{\mathrm{d}U}=\begin{pmatrix} 0 & 0 & 1\\ -\dfrac{\kappa em}{\rho^2}+(\kappa-1)\dfrac{m^3}{\rho^3} & \dfrac{\kappa m}{\rho} & \dfrac{\kappa e}{\rho}-\tfrac{3}{2}(\kappa-1)\dfrac{m^2}{\rho^2}\\ \tfrac{1}{2}(\kappa-3)\dfrac{m^2}{\rho^2} & \kappa-1 & -(\kappa-3)\dfrac{m}{\rho}\end{pmatrix}$$

The conservation law form is used for the numerical solution of the pipe equations (see next section).

For a complete description of the gas flow in the pipe (length L) we need initial values and boundary values in addition to (16). The boundary values are functions of the cylinder values on one side and atmospheric gas properties on the other as discussed later. For the model description see Engl[4], Stark *et al.*[16].

NUMERICAL METHODS

An o.d.e. system with discontinuous right-hand side can be solved by a numerical method of high order together with switching functions in order to handle the discontinuities[1,12]. However, this technique does not seem suitable and efficient for the solution of the cylinder equations (1), (2), since the right-hand side of the o.d.e. system is based on too many empirical functions. Therefore the explicit first order method of Euler was used[17].

The hyperbolic system (16) describing the gas flow in the pipe was solved by a TVD method applied to the conservation law form (19), (20)

$$\frac{\partial U}{\partial t}+\frac{\partial F(U)}{\partial x}=0 \quad \text{or equivalently}$$

$$\frac{\partial U}{\partial t}+A(U)\frac{\partial U}{\partial x}=0, \qquad \text{where} \quad A(U)=\frac{\mathrm{d}F(U)}{\mathrm{d}U}$$

TVD (total variation diminishing) methods belong to the class of high resolution schemes for hyperbolic conservation laws. They produce numerical solutions whose total variation is non-increasing with time. Unwanted oscillations are prevented[8,10].

Our solution procedure is based on a second-order explicit 5-point TVD-method by Harten[6] who introduced the concept of total variation boundedness. In the following we present the scheme for a single conservation law

$$u_t+f(u)_x\equiv u_t+a(u)u_x=0, \qquad a(u)=\mathrm{d}f(u)/\mathrm{d}u, \qquad -\infty<x<\infty \tag{21}$$

with initial conditions given for $t=0$. Let u_j^n denote approximations to the exact solution u at discretization points (x_j, t_n), $j\in\mathbb{Z}, n\in\mathbb{N}$.

The TVD method is written in terms of a numerical flux function $\bar{f}$ which is *consistent* with the physical flux $f(\bar{f}(u,\ldots,u)=f(u))$:

$$u_j^{n+1}=u_j^n-r(\bar{f}_{j+\frac{1}{2}}^n-\bar{f}_{j-\frac{1}{2}}^n), \qquad r=\frac{\Delta t}{\Delta x}, \qquad j\in\mathbb{Z} \tag{22}$$

where

$\Delta t=t_{n+1}-t_n$: time step

$\Delta x=x_{j+1}-x_j$, $j\in\mathbb{Z}$: constant mesh width in x-direction

$$\bar{f}_{j+\frac{1}{2}}^n=\frac{1}{2}\left[f(u_j^n)+f(u_{j+1}^n)+\frac{1}{r}(g_j^n+g_{j+1}^n)-\frac{1}{r}Q(r\bar{a}_{j+\frac{1}{2}}^n+\gamma_{j+\frac{1}{2}}^n)\Delta_{j+\frac{1}{2}}^n u\right]$$

$$\Delta_{j+\frac{1}{2}}^n u=u_{j+1}^n-u_j^n$$

$$\bar{a}_{j+\frac{1}{2}}^n=\begin{cases}[f(u_{j+1}^n)-f(u_j^n)]/\Delta_{j+\frac{1}{2}}^n u & \text{for } \Delta_{j+\frac{1}{2}}^n u\neq 0\\ a(u_j^n) & \text{for } \Delta_{j+\frac{1}{2}}^n u=0\end{cases}$$

$$g_j^n=\mathrm{sgn}(\tilde{g}_{j+\frac{1}{2}}^n)\max[0,\min(|\tilde{g}_{j+\frac{1}{2}}^n|,\tilde{g}_{j-\frac{1}{2}}^n\,\mathrm{sgn}(\tilde{g}_{j+\frac{1}{2}}^n))]$$

$$\tilde{g}_{j+\frac{1}{2}}^n=\tfrac{1}{2}[Q(r\bar{a}_{j+\frac{1}{2}}^n)-(r\bar{a}_{j+\frac{1}{2}}^n)^2]\Delta_{j+\frac{1}{2}}^n u$$

$$\gamma_{j+\frac{1}{2}}^n=(g_{j+1}^n-g_j^n)/\Delta_{j+\frac{1}{2}}^n u$$

$$Q(x)=\begin{cases}\dfrac{x^2}{4\varepsilon}+\varepsilon, & |x|<2\varepsilon\\ |x|, & |x|\geqslant 2\varepsilon\end{cases}$$

$$\varepsilon=0.1$$

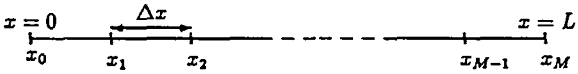

Figure 6 Discretization in pipe

The scheme is total variation diminishing under the CFL-like restriction

$$\max_j \left|\bar{a}^n_{j+\frac{1}{2}} \frac{\Delta t}{\Delta x}\right| \leqslant 1$$

The scalar scheme (22) can be extended to general systems of conservation laws as described by Harten[6], and the method was applied to the pipe equations (19), (20). In this case the CFL condition

$$\max_{i=1,2,3} \left|\lambda_i \frac{\Delta t}{\Delta x}\right| \leqslant 1 \tag{23}$$

has to be satisfied for each time step Δt, where λ_i, $i=1,2,3$, denote the eigenvalues of the matrix A in (20) or equivalently the characteristic slopes in (17). More precisely, let $x_0, x_1, \ldots, x_M$ be the discretization points in the inlet pipe as shown in *Figure 6*, and

$$\rho^n_j, u^n_j, p^n_j \text{ and } T^n_j, \qquad 0 \leqslant j \leqslant M$$

denote approximations of $\rho(x_j, t_n)$ and so on.

Assume that ρ, u, p and T are known for the time level t_n. The CFL condition (23) is satisfied, if the time step Δt and the new time level $t_{n+1}=t_n+\Delta t$ are restricted by:

$$\Delta t \leqslant \frac{\Delta x}{MAX} \tag{24}$$

where

$$MAX = \max_{0 \leqslant j \leqslant M} (|u^n_j| + a^n_j), \qquad a^n_j = \sqrt{\kappa \frac{p^n_j}{\rho^n_j}}$$

Experiments were also made with the Lax–Wendroff method applied to the pipe equations, see Engl and Rentrop[5]. The Lax–Wendroff method is based on a standard finite difference discretization of (19), (20), see e.g. Hirsch[8], LeVeque[10]. Note that the method is obtained by choosing $Q(x)=x^2$ in (22). Our results are in good agreement with the fact that schemes of this type produce spurious oscillations in the numerical solution. The TVD method leads to smoother solutions.

THE COUPLING PROBLEM

We now study the coupling of the systems cylinder and inlet pipe on one side, inlet pipe and atmosphere on the other.

The mentioned numerical methods are applied by using uniform discretization in the pipe (Δx=const.) and variable time steps Δt. *Figure 7* shows the situation for two time levels. The coupling quantities are equivalent to the boundary values of the pipe equations, i.e. we have

$$\rho^K_{ZE} = \rho_E(x_0), \qquad u^K_{ZE} = u_E(x_0), \qquad p^K_{ZE} = p_E(x_0), \qquad T^K_{ZE} = T_E(x_0)$$

for the coupling cylinder-pipe and

$$\rho^K_{ATE} = \rho_E(x_M), \qquad u^K_{ATE} = u_E(x_M), \qquad p^K_{ATE} = p_E(x_M), \qquad T^K_{ATE} = T_E(x_M)$$

for the coupling pipe-atmosphere.

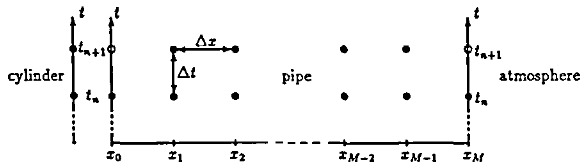

Figure 7 Discretization

In the following the subscript 'E' for the pipe values is omitted. Let

$$\rho_j^n, u_j^n, p_j^n, T_j^n \qquad 0 \leqslant j \leqslant M \qquad \text{and } \rho_Z^n, p_Z^n, T_Z^n$$

denote approximate values for the solution of the pipe equations at grid points (x_j, t_n) and for the cylinder values at time $t = t_n$.

Applying the explicit numerical methods described above to the cylinder and pipe equations we obtain approximate values

$$\rho_j^{n+1}, u_j^{n+1}, p_j^{n+1}, T_j^{n+1} \qquad 1 \leqslant j \leqslant M-1 \qquad \text{and } \rho_Z^{n+1}, p_Z^{n+1}, T_Z^{n+1}$$

at time $t_{n+1} = t_n + \Delta t$.

In order to find the unknowns at meshpoints (x_0, t_{n+1}) and (x_M, t_{n+1}) we need suitable coupling conditions. We present different coupling methods which are discussed separately for the coupling pipe–atmosphere and for the coupling cylinder–pipe in the following subsections.

Coupling pipe-atmosphere

In this case we need equations for the unknowns

$$\rho_M^{n+1}, u_M^{n+1}, p_M^{n+1} \text{ and } T_M^{n+1}$$

The number of physical boundary conditions to be imposed corresponds to the number of characteristics with negative slope at (x_M, t_{n+1}). In addition, numerical boundary conditions are required for a complete system of three boundary equations. More details about the boundary treatment of the pipe equations (Euler equations) can for example be found in Hirsch[8]. The assumption of subsonic flow ($|u| < a$) is reasonable for the following.

Quasi-steady method. Neglecting time dependence at time $t = t_{n+1}$ and assuming isentropic flow ($p\rho^{-\kappa} = \text{const.}$) and conservation of enthalpy ($c_p T + u^2/2 = \text{const.}$) we obtain for the case $p_{M-1} \leqslant p_{AT}$ (inflow)

$$\begin{aligned} p_M &= p_{M-1} \\ T_M &= T_{AT}\left(\frac{p_M}{p_{AT}}\right)^{(\kappa-1)/\kappa} \\ u_M &= -\sqrt{2c_p(T_{AT} - T_M)} \end{aligned} \tag{25}$$

and for the case $p_{M-1} > p_{AT}$ (outflow)

$$\begin{aligned} p_M &= p_{AT} \\ T_M &= T_{M-1}\left(\frac{p_M}{p_{M-1}}\right)^{(\kappa-1)/\kappa} \\ u_M &= \sqrt{u_{M-1}^2 + 2c_p(T_{M-1} - T_M)} \end{aligned} \tag{26}$$

(the upper index '$n+1$' is omitted). Concerning physical boundary conditions, $p\rho^{-\kappa}$ and $c_p T + u^2/2$ are prescribed in the inflow case, and p is imposed in the outflow case. The numerical boundary conditions are obtained by extrapolation of inner values. ρ_M is determined by the ideal gas law: $\rho_M = p_M/RT_M$. Since the atmospheric values are given at any time, we can easily solve these equations for the unknowns.

Method of characteristics. We now use the characteristic form (18) of the pipe equations:

$$(p_t + (u+a)p_x) + \rho a(u_t + (u+a)u_x) = 0$$
$$(p_t + (u-a)p_x) - \rho a(u_t + (u-a)u_x) = 0$$
$$(p_t + up_x) - a^2(\rho_t + u\rho_x) = 0$$

with its characteristic slopes

$$\lambda_1 = u+a, \qquad \lambda_2 = u-a \qquad \text{and} \quad \lambda_3 = u$$

Courant *et al.*[3] suggested a difference method for the solution of a hyperbolic system which is written in characteristic form: All time derivatives are replaced by forward difference quotients, and in each equation the space derivatives are replaced by backward (forward) difference quotients if the corresponding characteristic slope is positive (negative).

Using this idea in our case at $x = x_M$ and assuming $|u| < a$ we find

$$\frac{p_M^{n+1} - p_M^n}{\Delta t} + (u+a)_M^n \frac{p_M^n - p_{M-1}^n}{\Delta x} + (\rho a)_M^n \left(\frac{u_M^{n+1} - u_M^n}{\Delta t} + (u+a)_M^n \frac{u_M^n - u_{M-1}^n}{\Delta x} \right) = 0$$
$$\frac{p_M^{n+1} - p_M^n}{\Delta t} + (u-a)_M^n \frac{p_{AT} - p_{M-1}^n}{\Delta x} - (\rho a)_M^n \left(\frac{u_M^{n+1} - u_M^n}{\Delta t} + (u-a)_M^n \frac{u_{AT} - u_{M-1}^n}{\Delta x} \right) = 0$$

and

$$\frac{p_M^{n+1} - p_M^n}{\Delta t} + u_M^n \frac{p_M^n - p_{M-1}^n}{\Delta x} - (a^2)_M^n \left(\frac{\rho_M^{n+1} - \rho_M^n}{\Delta t} + u_M^n \frac{\rho_M^n - \rho_{M-1}^n}{\Delta x} \right) = 0 \tag{27}$$

for $u_M^n > 0$ or

$$\frac{p_M^{n+1} - p_M^n}{\Delta t} - (a^2)_M^n \frac{\rho_M^{n+1} - \rho_M^n}{\Delta t} = 0$$

for $u_M^n = 0$ or

$$\frac{p_M^{n+1} - p_M^n}{\Delta t} + u_M^n \frac{p_{AT} - p_{M-1}^n}{\Delta x} - (a^2)_M^n \left(\frac{\rho_M^{n+1} - \rho_M^n}{\Delta t} + u_M^n \frac{\rho_{AT} - \rho_{M-1}^n}{\Delta x} \right) = 0$$

for $u_M^n < 0$.

The numerical as well as physical boundary conditions are now obtained by a discretization of the characteristic equations. System (27) has the form

$$\begin{aligned} a_1 p_M^{n+1} + b_1 u_M^{n+1} + c_1 &= 0 \\ a_1 p_M^{n+1} - b_1 u_M^{n+1} + c_2 &= 0 \\ a_1 p_M^{n+1} + b_3 \rho_M^{n+1} + c_3 &= 0 \end{aligned} \tag{28}$$

with known coefficients $a_1, b_1, \ldots, c_3$ and can therefore be solved for the unknowns p_M^{n+1}, u_M^{n+1} and ρ_M^{n+1}. T_M^{n+1} is given by the ideal gas law. Note that a negative characteristic slope in the original equations (18) introduces the atmospheric values.

Combination of the quasi-steady method and the method of characteristics. The quasi-steady method does not take into account the characteristic equations but uses an extrapolation technique to obtain numerical boundary conditions. The method of characteristics, however, considers characteristic curves with positive as well as negative slope and assumes some kind of continuation of the curves into the region outside the pipe. We suggest a third method which combines the ideas of both methods described above and seems to be a better approach:

We only consider the equations of the characteristic form (18) with positive characteristic slope and replace the partial derivatives by difference quotients according to the method of characteristics. This yields numerical boundary conditions. The system of coupling conditions is completed by steady-flow boundary conditions which correspond to the physical boundary conditions of the quasi-steady method[13].

We obtain the following system of equations in the case of inflow ($u_M^n \leq 0$):

$$\begin{aligned} c_p T_M^{n+1} + \frac{(u_M^{n+1})^2}{2} &= c_p T_{AT} \quad \text{(conservation of enthalpy)} \\ p_M^{n+1}(\rho_M^{n+1})^{-\kappa} &= p_{AT}\rho_{AT}^{-\kappa} \quad \text{(isentropic flow)} \\ a_1 p_M^{n+1} + b_1 u_M^{n+1} + c_1 &= 0 \quad \text{(1st equation in (28))} \end{aligned} \tag{29}$$

In the case of outflow ($u_M^n > 0$) we have

$$\begin{aligned} \rho_M^{n+1} &= \rho_{AT} \\ a_1 p_M^{n+1} + b_1 u_M^{n+1} + c_1 &= 0 \quad \text{(1st equation in (28))} \\ a_1 p_M^{n+1} + b_3 \rho_M^{n+1} + c_3 &= 0 \quad \text{(3rd equation in (28))} \end{aligned} \tag{30}$$

The first system can be transformed into a non-linear equation for ρ_M^{n+1} which was solved using Newton's method. System (30) is linear, and the solution can easily be obtained.

Coupling cylinder-pipe

Instead of presenting a satisfying solution for the coupling cylinder–pipe (which has not yet been found), we will describe the approaches made so far and mention the difficulties which arose. Numerical results show that the coupling problem cannot be neglected and a proper treatment of the coupling conditions is very important. As in the case of the coupling pipe–atmosphere different coupling methods for finding the unknowns

$$\rho_0^{n+1},\ u_0^{n+1},\ p_0^{n+1},\ T_0^{n+1}$$

are presented. Again, subsonic flow is assumed ($|u| < a$).

Quasi-steady method. In addition to the assumptions of steady and isentropic flow and conservation of enthalpy we distinguish the cases of an open and a closed inlet valve and obtain at time $t = t_{n+1}$ (the upper index '$n+1$' is omitted):

- Open inlet valve ($A_E(t_{n+1}) \neq 0$)
  $p_1 \leq p_Z$ (inflow into pipe)

$$\begin{aligned} p_0 &= p_1 \\ T_0 &= T_Z\left(\frac{p_0}{p_Z}\right)^{(\kappa-1)/\kappa} \\ u_0 &= \sqrt{2c_p(T_Z - T_0)} \end{aligned} \tag{31}$$

  $p_1 > p_Z$ (outflow from pipe)

$$\begin{aligned} p_0 &= p_Z \\ T_0 &= T_1\left(\frac{p_0}{p_1}\right)^{(\kappa-1)/\kappa} \\ u_0 &= -\sqrt{u_1^2 + 2c_p(T_1 - T_0)} \end{aligned} \tag{32}$$

- Closed inlet valve ($A_E(t_{n+1})=0$)

$$
\begin{aligned}
&u_0=0\\
&T_0=T_1+\frac{u_1^2}{2c_p}\\
&p_0=p_1\left(\frac{T_1}{T_0}\right)^{\kappa/(1-\kappa)}
\end{aligned}
\tag{33}
$$

The ideal gas law yields $\rho_0=p_0/RT_0$. Note that T_Z and p_Z are obtained as solutions of the o.d.e. system.

Method of characteristics. We use the characteristic form (18) of the pipe equations and replace the time derivatives by forward difference quotients and the space derivatives in each equation by backward or forward difference quotients depending on the slope of the corresponding characteristic curve. With the assumption $|u|<a$ we find for the case of an open inlet valve ($A_E(t_{n+1})\neq 0$):

$$
\frac{p_0^{n+1}-p_0^n}{\Delta t}+(u+a)_0^n\frac{p_1^n-p_Z^n}{\Delta x}+(\rho a)_0^n\left(\frac{u_0^{n+1}-u_0^n}{\Delta t}+(u+a)_0^n\frac{u_1^n-u_Z^n}{\Delta x}\right)=0
$$

$$
\frac{p_0^{n+1}-p_0^n}{\Delta t}+(u-a)_0^n\frac{p_1^n-p_0^n}{\Delta x}-(\rho a)_0^n\left(\frac{u_0^{n+1}-u_0^n}{\Delta t}+(u-a)_0^n\frac{u_1^n-u_0^n}{\Delta x}\right)=0
$$

and

$$
\frac{p_0^{n+1}-p_0^n}{\Delta t}+u_0^n\frac{p_1^n-p_Z^n}{\Delta x}-(a^2)_0^n\left(\frac{\rho_0^{n+1}-\rho_0^n}{\Delta t}+u_0^n\frac{\rho_1^n-\rho_Z^n}{\Delta x}\right)=0 \tag{34}
$$

for $u_0^n>0$ or

$$
\frac{p_0^{n+1}-p_0^n}{\Delta t}-(a^2)_0^n\frac{\rho_0^{n+1}-\rho_0^n}{\Delta t}=0
$$

for $u_0^n=0$ or

$$
\frac{p_0^{n+1}-p_0^n}{\Delta t}+u_0^n\frac{p_1^n-p_0^n}{\Delta x}-(a^2)_0^n\left(\frac{\rho_0^{n+1}-\rho_0^n}{\Delta t}+u_0^n\frac{\rho_1^n-\rho_0^n}{\Delta x}\right)=0
$$

for $u_0^n<0$.

This system has the form

$$
\begin{aligned}
&\tilde{a}_1p_0^{n+1}+\tilde{b}_1u_0^{n+1}+\tilde{c}_1=0\\
&\tilde{a}_1p_0^{n+1}-\tilde{b}_1u_0^{n+1}+\tilde{c}_2=0\\
&\tilde{a}_1p_0^{n+1}+\tilde{b}_3\rho_0^{n+1}+\tilde{c}_3=0
\end{aligned}
\tag{35}
$$

where the coefficients $\tilde{a}_1,\tilde{b}_1,\ldots,\tilde{c}_3$ are known.

In the case of a closed inlet valve ($A_E(t_{n+1})=0$) we have $u_0^{n+1}=0$, and the approximations of the 2nd and 3rd characteristic equations yield $\tilde{a}_1p_0^{n+1}+\tilde{c}_2=0$ and $\tilde{a}_1p_0^{n+1}+\tilde{b}_3\rho_0^{n+1}+\tilde{c}_3=0$ (see (34), (35)). Note that in this case the equations are not dependent on the physical properties of the cylinder.

Remarks. We have already mentioned critical aspects of the quasi-steady method and the method of characteristics. For the coupling pipe–atmosphere we obtained a better approach by combining the two methods. The implementation of a combined approach for the coupling cylinder–pipe, however, lead to instabilities expressed by negative approximate values for the pipe pressure.

Further investigations will be based on the pipe equations (15) by which a variable cross-sectional area within a region of the boundary can be taken into account.

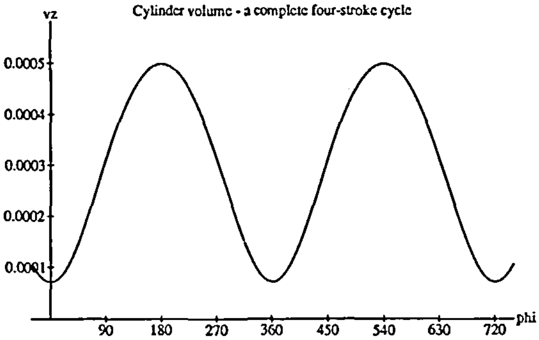

Figure 8 Cylinder volume $V_z[\mathrm{m}^3]$ *versus* crank angle $\varphi(\varphi=\omega t)$

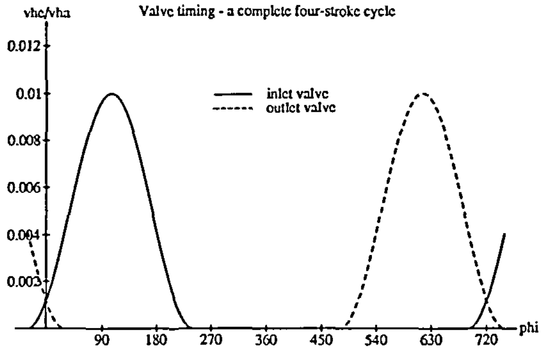

Figure 9 Valve timing $vh_E/vh_A[\mathrm{m}]$ *versus* crank angle $\varphi(\varphi=\omega t)$

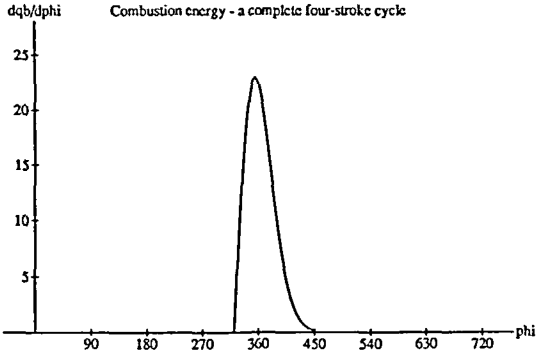

Figure 10 Combustion energy $\frac{\mathrm{d}Q_B}{\mathrm{d}\varphi}\left[\frac{J}{\text{crank angle}}\right]$ *versus* crank angle $\varphi(\varphi=\omega t)$

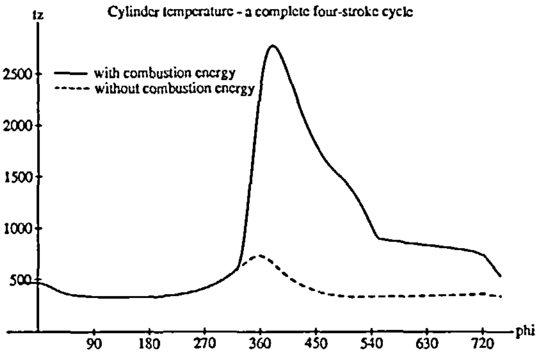

Figure 11 Cylinder temperature $T_z[\mathrm{K}]$ *versus* crank angle $\varphi(\varphi=\omega t)$

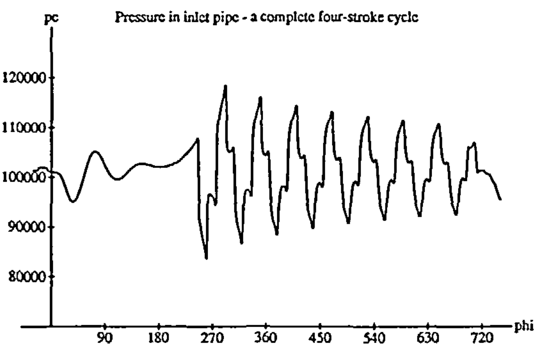

Figure 12 Pressure $p_E(\mathrm{N/m}^2)$ for fixed $x=L/2$ in the inlet pipe *versus* crank angle φ

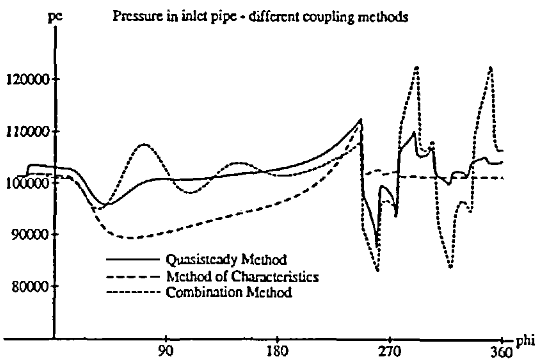

Figure 13 Pressure $p_E(\mathrm{N/m}^2)$ for fixed $x=L/2$ in the inlet pipe *versus* crank angle φ

NUMERICAL RESULTS

Illustrations and discussion

The first five of the presented figures show technically interesting results, the last one illustrates numerical aspects. The number of discretization intervals used in the inlet pipe is $M=80$.

Figure 8–12 refer to a complete four-stroke cycle which includes the inflow of a fresh fuel–air mixture through the inlet valve, combustion and the outflow of the burnt gas through the outlet valve.

The time dependencies of the cylinder volume, the valve opening/closing and the combustion energy are given as shown in *Figures 8–10.*

Figure 11 presents numerical results for the temperature in the cylinder. If no combustion energy is added, a lower temperature is obtained as depicted for comparison. The pressure in the inlet pipe as a function of t for fixed $x=L/2$ is shown in *Figure 12.* Note the oscillating behaviour of the pressure after closing the inlet valve.

The method of characteristics and the combination method were used for the coupling cylinder–pipe and the coupling pipe–atmosphere respectively. 7076 time steps were carried out.

Figure 13 refers to numerical properties. It shows the pressure in the inlet pipe as a function of t for fixed $x=L/2$ during one charge cycle. The numerical results were obtained by different coupling methods for the coupling pipe–atmosphere. The systems cylinder and pipe were coupled by the method of characteristics. In each case 3537 times steps were carried out.

Experiments were also made with non-reflecting boundary conditions for the open end of the pipe[7]. The results are very similar to the numerical solution which corresponds to a coupling of pipe and atmosphere by the method of characteristics. *Figure 13* clearly shows the main result of our work: the numerical solution of the cylinder and pipe equations is strongly dependent on the coupling conditions. On one side, many different ways of obtaining boundary values for the Euler equations are known[8]. On the other side, different boundary treatments do not necessarily yield similar numerical solutions as illustrated by our results. In our case, a proper treatment of the coupling problem is very important, and further work is being done.

Comparison with other studies

A similar modelling of the gas flow in an internal combustion engine can be found in Stark *et al.*[16], Lakshminarayanan *et al.*[9] In both cases, the numerical simulation involves standard finite difference schemes, and the coupling/boundary conditions are based on a quasi-steady approach. The papers do not include further studies on the influence of coupling conditions.

Concerning industrial applications, the program system PROMO and its improved version PROMO 2 are used in the German car industry. PROMO simulates the gas flow in an internal combustion engine, see Seifert *et al.*[15] Its mathematical model is similar to the model described in this paper. It involves one-dimensional treatment of the gas flow in the engine pipes and the modelling of cylinders by o.d.e. systems in time t. Experiments showed that a realistic model is obtained. The numerical solution procedure includes a Lax–Wendroff type method applied to the pipe equations. It is reported that, in general, a comparison between measurement and computation yields good results. However, in some cases it was observed that the Lax–Wendroff type scheme produced unacceptable numerical errors[14].

The boundary and coupling conditions in PROMO are imposed similarly to the combination method described in this paper. Numerical coupling conditions are obtained by a discretization of characteristic equations. Quasi-steady flow assumptions yield physical boundary conditions. More precisely, a steady flow equation by Saint Venant is used which determines the ideal mass flow m_{th} through a throttling point in a pipe. Momentum and energy losses are taken into account by a flow coefficient $\alpha\,(0\leqslant\alpha\leqslant 1)$: αm_{th} denotes the real mass flow. The flow coefficient is determined by measurement, and the user of PROMO has to provide flow coefficients for all points of the engine where boundary/coupling conditions are required. If the physical boundary conditions of the combination method are replaced by the engineers' equations which involve the flow coefficient α, similar results are obtained with a choice of α close to 1 (*Figure 14*). However, the non-linear system of coupling equations becomes a lot more complex.

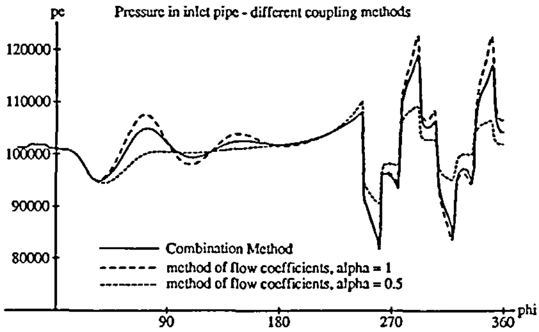

Figure 14 Pressure p_E(N/m^2) for fixed $x=L/2$ in the inlet pipe *versus* crank angle φ

Figure 14 refers to the model described in this paper. It shows the pressure in the inlet pipe as a function of t for fixed $x=L/2$ during one charge cycle. The numerical results were obtained by different coupling methods for the coupling pipe–atmosphere. The solid line corresponds to the presented combination method, and the PROMO approach yields results represented by the broken lines.

ACKNOWLEDGEMENTS

We are deeply indebted to the Laboratory of Technomathematics of H. Neunzert at the University of Kaiserslautern. We thank our colleagues of the Numerical Mathematics group of R. Bulirsch at the TU München for helpful discussions.

REFERENCES

1 Bulirsch, R. *Die Mehrzielmethode zur numerischen Lösung von nichtlinearen Randwertproblemen und Aufgaben der optimalen Steuerung.* Vortrag im Lehrgang Flugbahnoptimierung der Carl-Cranz Gesellschaft (Oktober 1971)
2 Chorin, A. J. and Marsden, J. E. *A Mathematical Introduction to Fluid Mechanics,* Springer, Berlin (1979)
3 Courant, R., Isaacson, E. and Rees, M. On the solution of nonlinear hyperbolic differential equations by finite differences, *Commun. Pure Appl. Math.*, 5, 213–255 (1952)
4 Engl, G. Mathematische Modellbildung und numerische Studien beim Verbrennungsmotor, *Diplomarbeit,* Mathematisches Institut, Technische Universität München (August 1989)
5 Engl, G. and Rentrop, P. Case studies for a single cylinder combustion engine. *Proc. ECMI V* (Ed. M. Heiliö), Teubner–Kluwer, pp. 217–222 (1991)
6 Harten, A. High resolution schemes for hyperbolic conservation laws, *J. Comput. Phys.*, 49, 357–393 (1983)
7 Hedstrom, G. W. Nonreflecting boundary conditions for nonlinear hyperbolic systems, *J. Comput. Phys.*, 30, 222–237 (1979)
8 Hirsch, C., *Numerical Computation of Internal and External Flows,* Vol. 2, John Wiley, Chichester (1990)
9 Lakshminarayanan, P. A., Janakiraman, P. A., Gajendra Babu, M. K. and Murthy, B. S., Prediction of gas exchange processes in a single cylinder internal combustion engine, *SAE Paper 790359* (1979)
10 LeVeque, R. J. *Numerical Methods for Conservation Laws,* Birkhäuser, Basel (1990)
11 Majda, A. *Compressible Fluid Flow and Systems of Conservation Laws in Several Space Variables,* Springer, Berlin (1984)
12 Rentrop, P. *Unterlagen zum Carl-Cranz Kurs V1.18, Rechenverfahren und Programme für die Bewegungsgleichungen mechanischer Systeme,* Oberpfaffenhofen bei München (1987)
13 von Rosenberg, D. U., Beauchamp, D. L. and Watts, J. W. An efficient numerical solution of non-linear hyperbolic equations with split boundary conditions, *Chem. Eng. Sci.* 23, 345–351 (1968)
14 Seifert, H. A mathematical model for simulation of processes in an internal combustion engine, *Acta Astronaut.*, 6, 1361–1376 (1976)
15 Seifert, H. *et al.*, *Beschreibung des Programmsystems PROMO 2,* Forschungsberichte Verbrennungskraftmaschinen, *Reports 281-1, 281-2, 281-3,* Ruhr-Universität Bochum (1981)
16 Stark, H.-G., Trinkaus, H. and Jansson, Ch. *The Simulation of the Charge Cycle in a Cylinder of a Combustion Engine,* Berichte der Arbeitsgruppe Technomathematik, Bericht No. 31, Universität Kaiserslautern (September 1988)
17 Stoer, J. and Bulirsch, R. *Introduction to Numerical Analysis,* Springer, New York (1980)
18 Woschni, G. and Anisitis, F. Eine Methode zur Vorausberechnung der Änderung des Brennverlaufs mittelschnellaufender Dieselmotoren bei geänderten Betriebsbedingungen, *MTZ,* 34, 106–115 (1973)
19 Woschni, G. and Fieger, J. Experimentelle Bestimmung des örtlich gemittelten Wärmeübergangskoeffizienten im Ottomotor, *MTZ,* 42, 229–234 (1981)

APPENDIX: LISTING OF PHYSICAL PARAMETERS

Cylinder

cylinder diameter	$d=0.08\,[\mathrm{m}]$
length of stroke	$H=0.085\,[\mathrm{m}]$
length of connecting-rod	$l=0.17\,[\mathrm{m}]$
stroke volume	$V_H=4.2726\times 10^{-4}\,[\mathrm{m}^3]$
compression ratio	$\varepsilon=7$
length of crank	$r=0.0425\,[\mathrm{m}]$
ratio of r and l	$\lambda=\frac{r}{l}=0.25$
number of revolutions per second	$nu=17\left[\frac{1}{\mathrm{sec}}\right]$
average surface temperature	$T_W=450\,[\mathrm{K}]$

Valves

diameters	$d_E=0.036\,[\mathrm{m}]$
	$d_A=0.028\,[\mathrm{m}]$
angle	$\beta=\frac{\pi}{4}$

Inlet pipe

length of inlet pipe	$L=1.0\,[\mathrm{m}]$

Thermodynamic constants

universal gas constant	$R=287\left[\frac{\mathrm{J}}{\mathrm{kg\,K}}\right]$
specific heat capacities	$c_v=718\left[\frac{\mathrm{J}}{\mathrm{kg\,K}}\right]$
	$c_p=1005\left[\frac{\mathrm{J}}{\mathrm{kg\,K}}\right]$
ratio of the specific heat capacities	$\kappa=1.4$

Atmosphere

pressure	$p_{AT}=1.013\times 10^5\left[\frac{\mathrm{N}}{\mathrm{m}^2}\right]$
temperature	$T_{AT}=300\,[\mathrm{K}]$
density	$\rho_{AT}=1.177\left[\frac{\mathrm{kg}}{\mathrm{m}^3}\right]$

Initial values (for $\varphi_i=-30°$ and $t_i=\varphi_i/\omega$)

cylinder pressure	$p_Z(t_i)=10^5\left[\frac{\mathrm{N}}{\mathrm{m}^2}\right]$
cylinder temperature	$T_Z(t_i)=470\,[\mathrm{K}]$
gas velocity in inlet pipe	$u_E(x,t_i)=0$ for $0\leqslant x\leqslant L$
pipe pressure	$p_E(x,t_i)=p_{AT}$ for $0\leqslant x\leqslant L$
pipe density	$\rho_E(x,t_i)=\rho_{AT}$ for $0\leqslant x\leqslant L$